Turkish Journal of Chemistry

http://journals.tubitak.gov.tr/chem/

Research Article

Turk J Chem
(2019) 43: 94 – 105

doi:10.3906/kim-1803-83

Preparation and physicochemical characterization of zinc oxide/sodium cellulose composite for food packaging

Sherif Mohamed Abdel Salam KESHK[1,2,*], **Mohamed Saad HAMDY**[1]

[1]Department of Chemistry, College of Science, King Khalid University, Abha, Saudi Arabia

[2]Department of Basic Science, Institute of Environmental Studies and Research, Ain Shams University, Abbassia, Cairo, Egypt

Received: 30.03.2018 • **Accepted/Published Online:** 15.10.2018 • **Final Version:** 05.02.2019

Abstract: Zinc oxide/sodium cellulose composite with different ZnO loadings was prepared for the first time. The crystal structures of cellulose, sodium cellulose, and ZnO/sodium cellulose composite were characterized by FT-IR, XRD, XPS, SEM, and EDX. ZnO/sodium cellulose showed a similar XRD pattern to that of cellulose II. The XPS spectrum emphasized the presence of Zn^{2+} and Na^{+} ions in the prepared composite. Additionally, the SEM analysis showed the growth of ZnO crystals on the sodium cellulose surface. UV-Vis spectrometry of the ZnO/sodium cellulose spectrum showed a distinguished absorption band at 360 nm that was attributed to the presence of ZnO particles on the cellulosic fibers. As a result, the composite fibers swelled, and their diameter increased from 15 µm to 30 µm. Furthermore, ZnO/sodium cellulose exhibited lower air and water vapor permeability than cellulose and sodium cellulose and can be perfectly utilized as food packing film to increase the shelf life of preserved foods.

Key words: Cellulose, sodium cellulose, composite, zinc oxide, permeability

1. Introduction

Food packaging is highly desirable to protect foodstuff from various exposures. New progress aims to increase the barrier properties to prevent microbiological infections of food.[1] Additionally, recyclable and renewable materials are considered to improve the sustainability of packaging via metal or polymer coatings, and hence various new polymers have been investigated.[2] Current developments in packaging material have focused on high barrier performance with a minimal amount of material.[3] Therefore, there is a need for functional coatings of cellulosic materials for special or enhanced properties in the field of food packaging. A magnetic nanoparticles (MNPS)/dialdehyde starch composite was fabricated for food packaging. The MNPs/dialdehyde starch composite films manifested lower water vapor transmission in comparison to dialdehyde starch film, so MNPs improved the hydrophobicity and mechanical properties of MNPs/dialdehyde starch composite films. Therefore, the prepared composite film was recommended for oxygen-sensitive foods like chilled meat, as it contains a highly effective oxygen scavenger (FeO).[2] Thus, the synthesis of metal oxide/cellulose composites has attracted considerable interest due to their interesting physical and chemical properties.[2–4] The morphology of cellulose composites, such as their size, shape, and crystallography, highly affects their properties.[4,5] Cellulose composites can replace conventional synthetic polymers in food and medical applications.[6,7] Zinc oxide is generally

*Correspondence: keshksherif@gmail.com

used in several applications, such as in the pharmaceutical, commodity chemical, and glass industries.[8–12] ZnO is currently listed as a safe food additive and preservative by the US Food and Drugs Administration. The reported synthetic methods of metal/cellulose composite preparation have poor metal stability in the composite and heterogeneous distributions of metals.[13–16] The preparation of metal/cellulose composites via the reduction of metal salts in aqueous suspensions of cellulose has been investigated.[17–19] In this method, a soluble metal salt is used with a suitable reducing agent in the presence of a costabilizer to avoid agglomeration and to improve the metal particle distribution on the cellulose.[20] Recently, microwave-assisted syntheses of metal/cellulose composites have been reported, in which ionic liquids were used to obtain cellulose fibers coated with metal particles.[21–23] On the other hand, the hydrophilicity of cellulose made it difficult to form a good composite with metals owing to hydrogen bonds between cellulose chains that hinder any other metal or metal oxide from forming a good composite.[22]

Sodium hydroxide treatment (mercerization) of natural cellulose (cellulose-$(OH)_3$) fibers results in the structural transformation to sodium cellulose (cellulose-$(ONa)_3$).[23,24] During mercerization, cellulose I proceeds through a crystal-to-crystal phase transformation. The intermediate structure between the parallel chains (cellulose I) and antiparallel chains (cellulose II) is sodium cellulose.[25] Sodium cellulose increases the interplanar distance between cellulose chains owing to O^-Na^+ group formation.[23–25] The mercerization affects the twisting and swelling of cellulose because of the presence of Na^+ ions, which play a crucial role in widening the accessible regions between the lattice planes to allow diffusion of the Na^+ ions into those planes.[25] The aluminum film is commonly used in food packaging because it has ideal barrier properties. However, its carbon footprint properties are totally lost at the highest humidity. Aluminum foil is ideal for wrapping foods and enables sealing out oxygen. However, it is not possible to view the contents of the bundle due to foil's opacity, it reacts with acidic foods, and it cannot be used inside microwave ovens. Aluminum reacts with oxygen to form a layer of aluminum oxide on the outside of the steel, so we cannot wrap food with it for a long time. Cellulose is inert but it is used to protect foods for short time intervals because it has poor barrier properties against air and moisture. In the current work, an effective synthetic technique was applied to prepare ZnO/sodium cellulose composites by using zinc acetate as a precursor for ZnO. The physicochemical characterization of ZnO/sodium cellulose is characterized by FT-IR spectroscopy, X-ray diffraction, XPS, and DTA analysis. Furthermore, ZnO/sodium cellulose permeability towards air and water vapor is evaluated.

2. Results and discussion

2.1. Composite characterizations

The FT-IR spectra of the cellulose, sodium cellulose, and ZnO/sodium cellulose composite were recorded in the range of 4000 to 400 cm^{-1} (Figure 2; Table 1). There are no significant differences in the FT-IR spectra for samples that were heated for various times. The inter- and intramolecular OH stretching vibration bands at 3440 cm^{-1} in the cellulose spectrum were completely flattened in the spectra of the sodium cellulose and the ZnO/sodium cellulose composite, which confirmed the transformation of the OH group to O^-Na^+ (Figure 1).[21–23] The peak at 1426 cm^{-1} in the cellulose spectrum, which is associated with both an intramolecular hydrogen bond at the C_6 group and the in-plane OH bending vibration, disappeared from spectra of both sodium cellulose and ZnO/sodium cellulose (Figure 1). Additionally, the peak at 1426 cm^{-1}, known as the "crystallinity band", decreased in both sodium cellulose and its composite due to the breakage of hydrogen bonding between the glycan chains in sodium cellulose.

These results showed that the ZnO/sodium cellulose composite has lower crystallinity than that of the sodium cellulose lattice structure. Moreover, the FT-IR spectrum of ZnO/sodium cellulose shows two strong absorption bands at 425 and 435 cm^{-1}, which were associated with the stretching vibrational bands of ZnO.[20] Furthermore, the spectrum had a weak peak at ~ 520 cm^{-1}, which is attributed to the vibrational mode of Zn–O.[20–22] Moreover, the peak at 2890 cm^{-1} can be attributed to CH_2 symmetric and asymmetric stretching. The intensity of this peak was found to decrease with ZnO loading as an indication of the presence of Zn ions in the lattice of sodium cellulose.

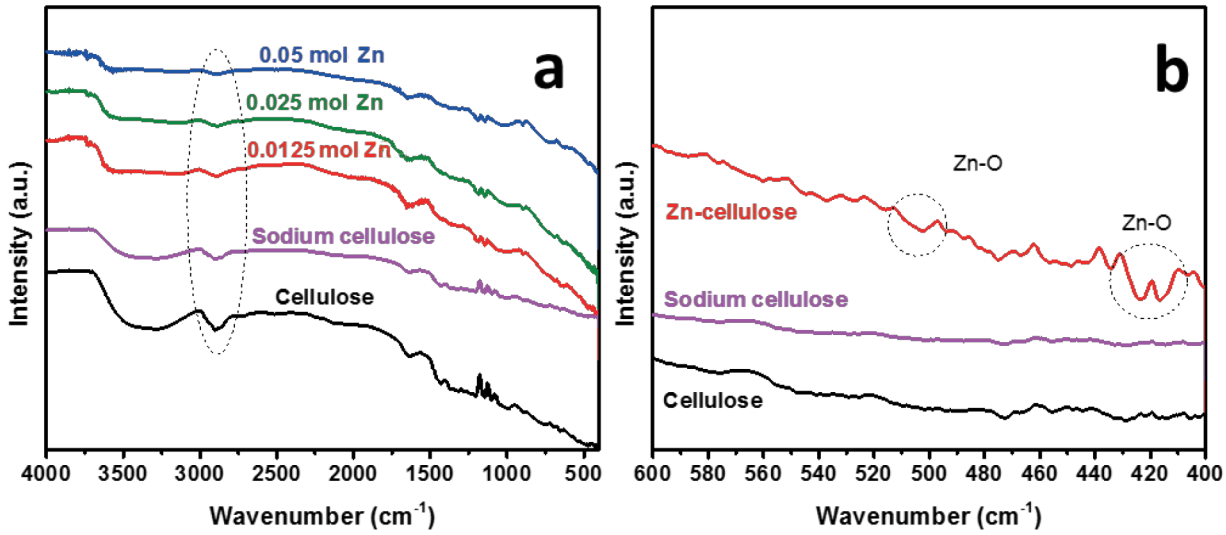

Figure 1. FT-IR spectra of cellulose, sodium cellulose, and ZnO/ sodium cellulose (a) at different ZnO loadings and (b) in the fine spectral range (400–600 cm^{-1}).

The crystal structure of the cellulose, sodium cellulose, and ZnO/sodium cellulose composite were investigated by X-ray diffractometry (Figures 2 and 3). The X-ray pattern of the cellulose exhibits the typical diffraction peaks of the crystalline structure of cellulose I at 2θ = 14.8°, 16.3°, 21.1°, and 22.5° (Figure 2).[26–28] However, the sodium cellulose sample exhibited the typical diffraction peaks of the crystalline structure of cellulose II at 2θ = 12.0°, 20.3°, and 21.5°. In addition, there were broad peaks at 34.8°and 41.4°, which correspond to the presence of sodium metal (Figure 2).[23–25] ZnO/sodium cellulose showed a similar XRD pattern to that of sodium cellulose (Figure 3). Additionally, the peaks at 2θ = 29.2°, 43.8°, 47.3°, and 48.3° represent the (100), (102), (112), and (201) lattice planes of ZnO, respectively (Figure 3).[26] This observation indicates a good distribution of zinc oxide within the hexagonal wurtzite structure. Moreover, no characteristic peaks were present to indicate the presence of zinc hydroxide.[26,27] The XRD data clearly indicate that ZnO particles are present within the sodium cellulose lattice.

Furthermore, the d-spacings corresponding to the ZnO/sodium cellulose peaks at 2θ = 12.0°, 20.3°, and 21.5° are significantly different compared with those of the sodium cellulose (Table 1). These results can be related to the good interaction between ZnO particles and sodium cellulose.

X-ray photoelectron spectroscopy (XPS) was performed to establish the presence of Na ions in the case of the ZnO/sodium cellulose composite (Figure 4). The pass energies for the survey scan and core level spectra were 100 and 60 eV, respectively, and are presented in Figure 4. The cellulose sample charges observed during

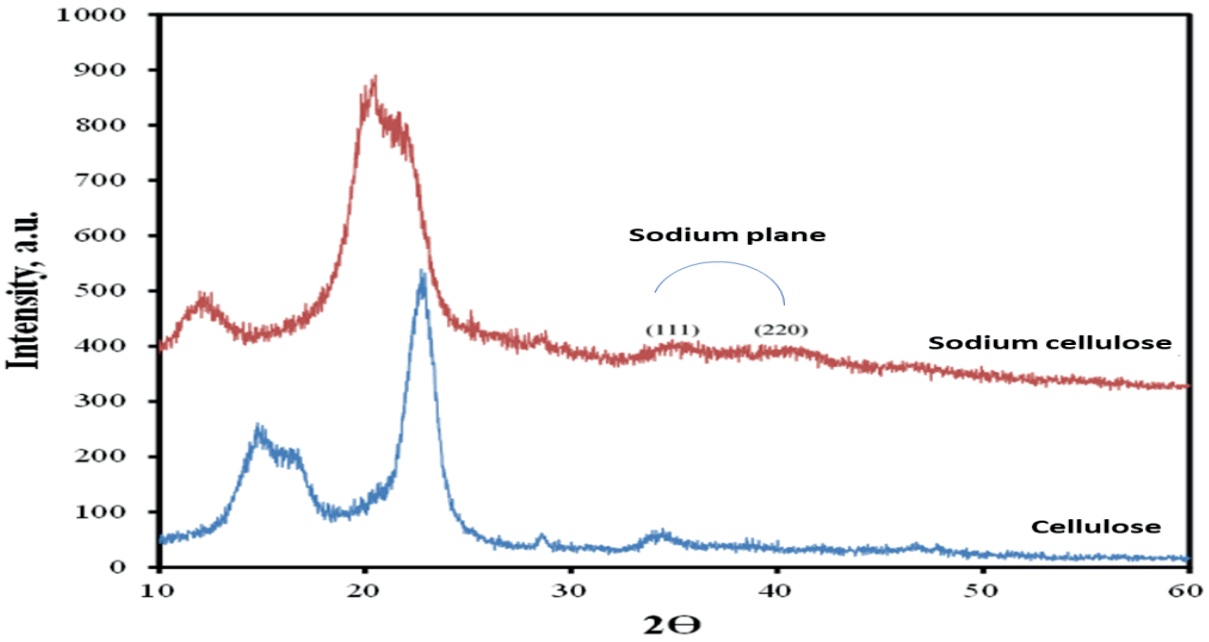

Figure 2. XRD pattern of cellulose compared to that of sodium cellulose.

Table 1. XRD analysis of cellulose and sodium cellulose compared with ZnO/sodium cellulose.

Sample	2θ / d (1 $\bar{1}$ 0)	2θ / d (1 1 0)	2θ / d (020)
Cellulose	14.8 (5.96)	16.2 (5.46)	22.7 (3.91)
Sodium cellulose	12.0 (7.35)	20.3 (4.36)	21.5 (4.11)
ZnO/sodium cellulose (30 min)	12.4 (7.14)	20.5 (4.32)	21.3 (4.16)

the photoemission studies were calibrated by assigning the C (1s) signal at 285 eV using an internal reference and the Fermi edge of the gold sample.

The survey spectrum of sodium cellulose shows sharp peaks for C (1s) (284.6 eV) and O (1s) (531 eV), whereas peaks related to Na^+ were observed at Na (1s) (1071 eV), Na (2s) (64 eV), and Na (2p) (31 eV). Furthermore, the spectrum of the ZnO/sodium cellulose composite (Figure 4) shows sharp peaks for C (1s) (284.6 eV), O (1s) (531 eV), Na(1s) (1071 eV), Na(2s) (64 eV), and Na(2p) (31 eV). Additionally, a strong peak was observed for Zn (2p) (1020 eV), which emphasized that both Na^+ and Zn^{2+} ions were present in the same phase.[28]

Scanning electron microscopy of the cellulose showed a cylindrical microstructure with a smooth surface and low variation in the diameter of the fiber, which was estimated to be 15 µm, without any unexpected phases (Figure 5). Nevertheless, the sodium cellulose swelled, with an average increase in the diameter to 20 µm. The micrographs of ZnO/sodium cellulose composite show the growth of ZnO crystals on the sodium cellulose surface (Figure 5), while the diameter of the fiber increased to an average of 26 µm.

Moreover, the micrographs clearly showed the effect of ZnO concentrations on the morphological structure of the ZnO/sodium cellulose composite. At low loadings of ZnO (i.e. <0.025 mol), ZnO particles exhibited a sphere-like uniform structure, while at high ZnO loading (i.e. >0.025 mol), the particles showed needle-like crystalline structure.

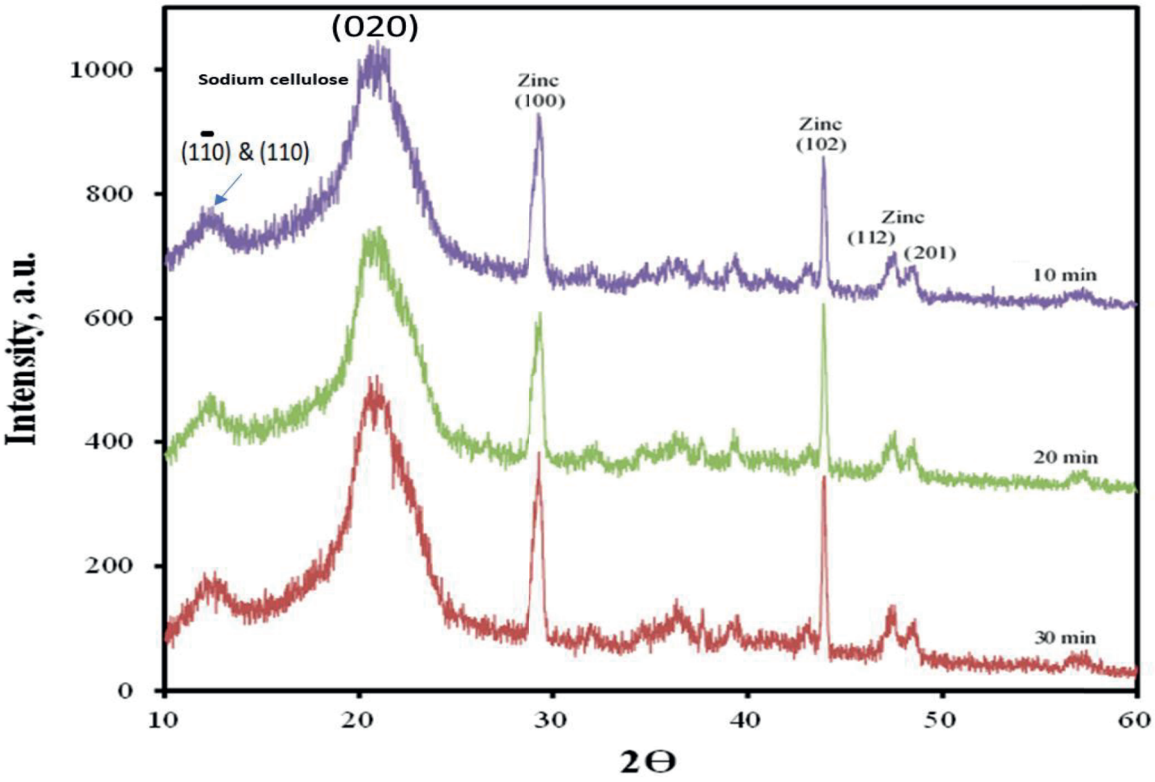

Figure 3. XRD patterns of ZnO/sodium cellulose composite prepared with different microwave heating times.

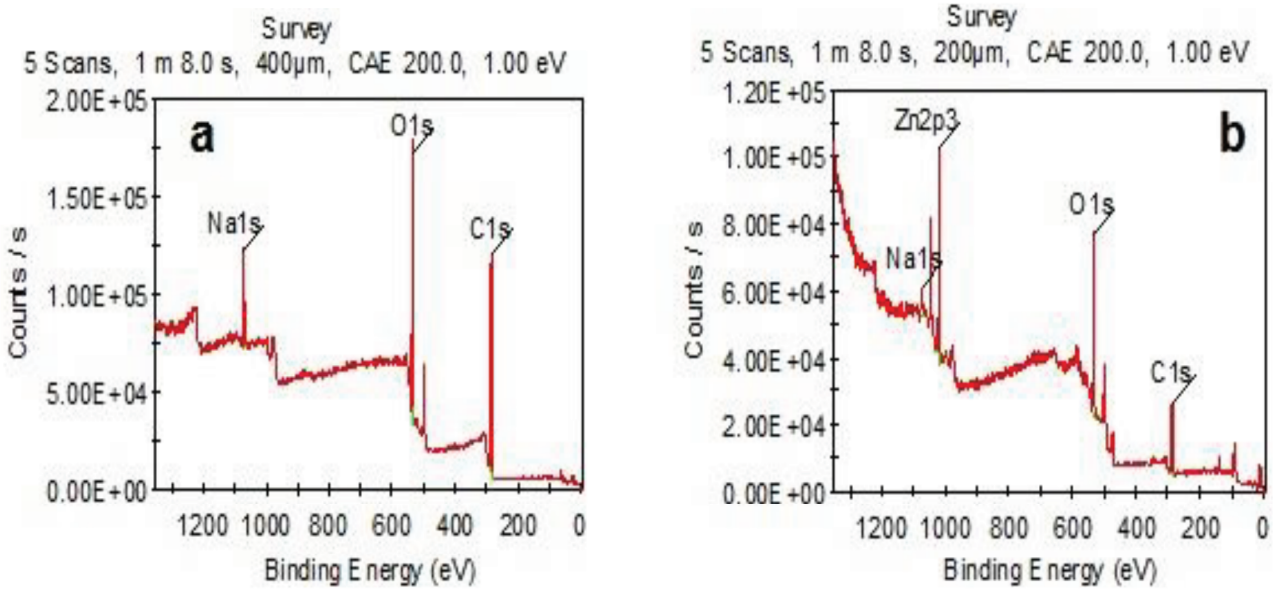

Figure 4. XPS survey scan spectra of (a) sodium cellulose and (b) ZnO/ sodium cellulose recorded with a photon energy of Al Kα (hv = 1486.6 eV).

EDX analysis was performed to investigate the elemental composition of the composite and to ensure the presence of Zn and Na ions (Figure 6). The EDX spectra exhibited various intense peaks that are associated with

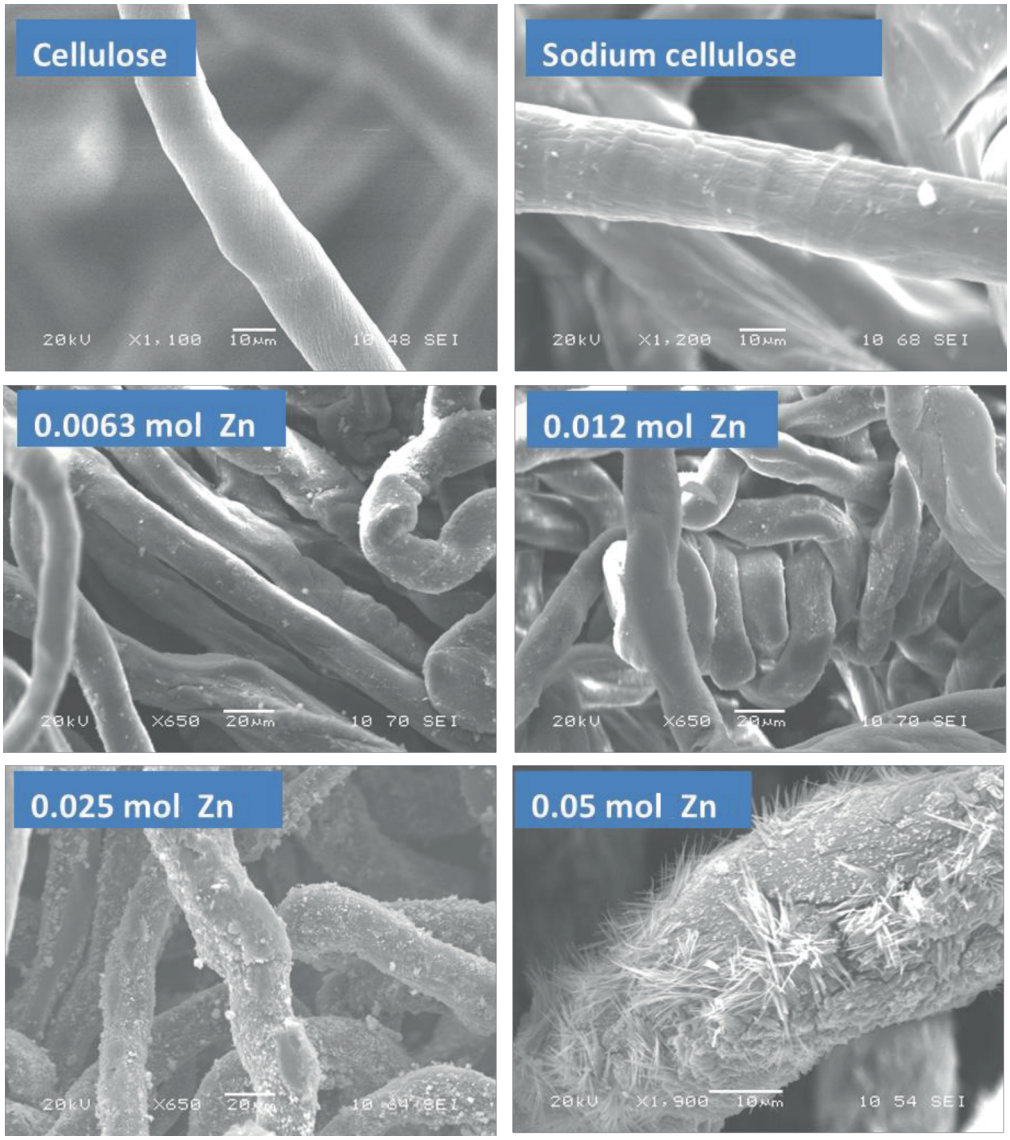

Figure 5. SEM micrographs of cellulose, sodium cellulose, and ZnO/sodium cellulose (at different levels of Zn-doping).

Zn, Na, O, and C atoms for the samples. Moreover, the presence of Zn and Na peaks in ZnO/sodium cellulose composite is clearly visible, which indicates the presence of ZnO particles in the sodium cellulose matrix.

UV-Vis spectrometry was used to investigate the optical properties of the ZnO/sodium cellulose composite with different amounts of zinc oxide, which were compared with the neat sodium cellulose (Figure 7). The composite spectra showed a distinguished absorption band at 360 nm that was absent in the sodium cellulose spectrum. This peak can be attributed to the presence of ZnO particles in the sodium cellulose. The absorption band showed a red shift compared with that of the commercial ZnO, which normally shows an absorption band at approximately 320–330 nm (Figure 7).

This shift is evidence of the strong interaction between the ZnO crystals and the sodium cellulose surface. This shift was showed previously due to the interaction between ZnO and a polymeric matrix.[28,29]

Characteristic thermal temperatures such as T_g, T_c, and T_p, were determined. From the DTA curves

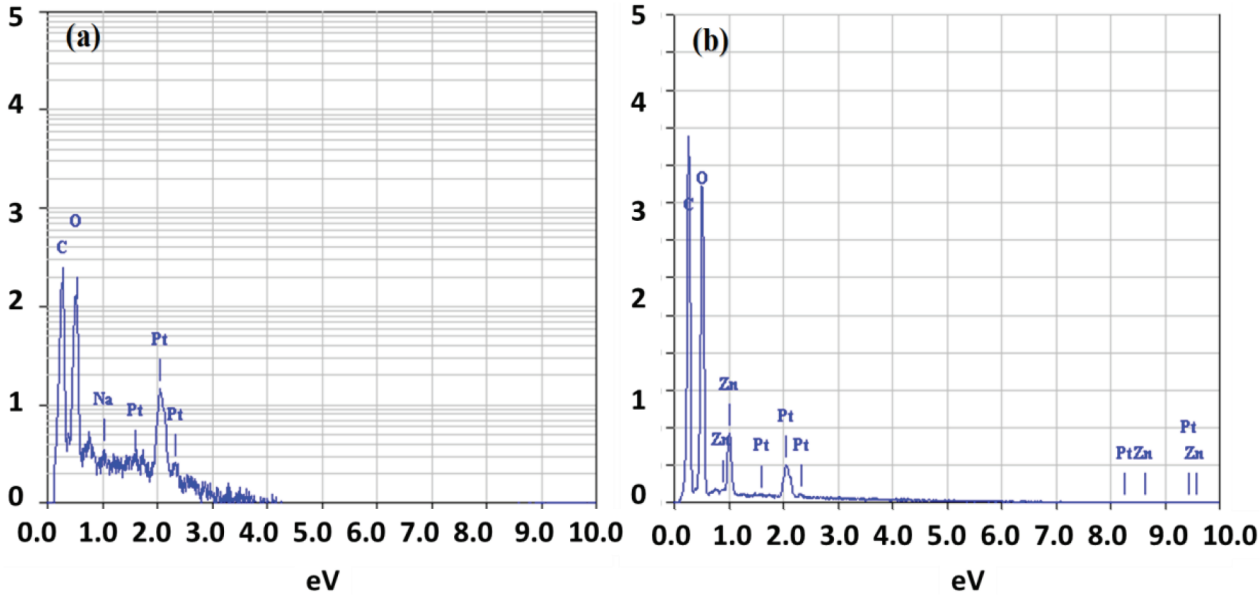

Figure 6. EDX analysis of (a) sodium cellulose and (b) ZnO/sodium cellulose.

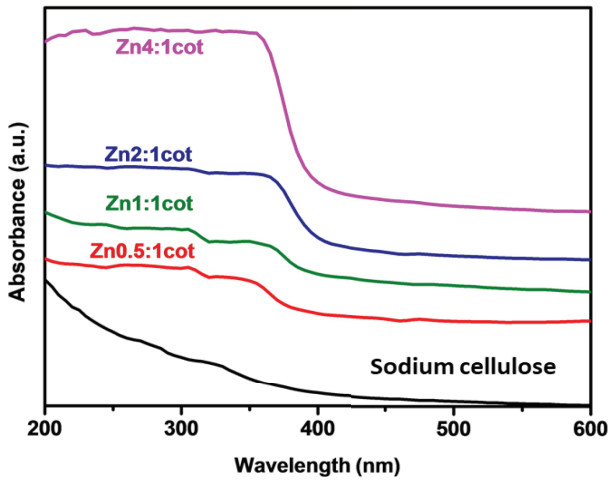

Figure 7. UV-Vis spectra of ZnO/sodium cellulose.

(Figure 8), the ZnO/sodium cellulose composite has higher T_g, T_c, and thermal stability compared with cellulose, sodium cellulose, and our last published data on NiO/sodium cellulose composite.[27] The T_g values are 55 °C, 76 °C, and 262 °C for cellulose, sodium cellulose, and ZnO/sodium cellulose, respectively (Figure 8). We can suggest that Zn ions were incorporated into the sodium cellulose matrix and created strong linkage bonds with higher binding energy, glass transition temperature, and thermal stability during the fabrication process in the application. These data do not agree with the published data on ZnO/cellulose composite that used microwave-assisted dissolution of cellulose in ionic liquid 1-butyl-3-methylimidazolium chloride,[30] because the presence of ZnO in the reported data was shown to be on the surface only. Furthermore, these reported data proved that the thermal stability of ZnO/cellulose was lower than that of regenerated cellulose due to the catalytic property of zinc oxide nanoparticles in the cellulose matrix.[30] In the current work, the ZnO crystals

are present on both the surface and the lattice structure of cellulose owing to the use of sodium cellulose.

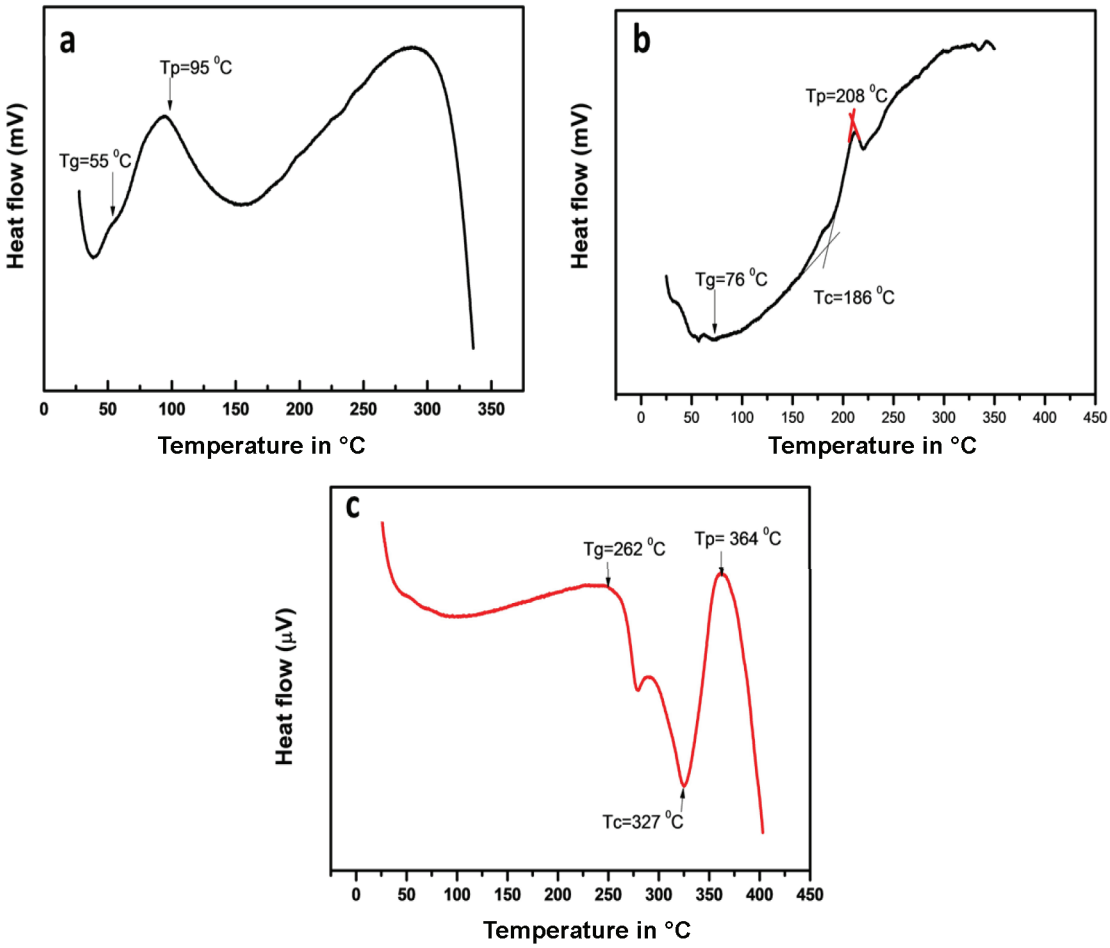

Figure 8. DSC profiles of (a) cellulose, (b) sodium cellulose, and (c) ZnO/sodium cellulose.

However, in the current work, the crystalline regions of sodium cellulose are bigger in size than the crystallites of cellulose I. Therefore, alkali cellulose is more reactive than cellulose I owing to the high interaction with ZnO.

2.2. Barrier properties of the composite

High barrier properties are the main goal for reducing the interaction of food with the outside air. Table 2 shows the water vapor transmission rate and air permeability of the fabricated composite. As a result of incorporating ZnO into sodium cellulose, the ability of air to pass through the composite is less than that in cellulose and sodium cellulose. The diffusion rate depends on the fraction of free volume cavities dynamically created in the cellulose matrix due to thermal motion of the cellulose chains. Incorporation of ZnO into the cellulose matrix creates a more tortuous path for the diffusing gas molecule than that encountered in neat cellulose. This can be explained by the morphology of the prepared composite. As seen in SEM, the cellulose showed a cylindrical microstructure with 15 µm diameter, whereas the sodium cellulose diameter increased to 20 µm. In the case of the composite the diameter becomes more dense than that in both cellulose and sodium cellulose (26 µm), which is sufficient to reduce the passage of air through the composite. In our previous reported results on lignosulfonate/sodium cellulose, the composite showed the highest water vapor transmission rate and air

permeability. Since lignosulfonate is an antioxidant and has high molecular weight, its barrier properties are not as good as in the case of ZnO.[31] The presence of the ZnO particles on the surface with a good distribution within the hexagonal wurtzite structure led to good fiber aggregation that improved barrier properties of the cellulose composite, where zinc oxide acts as a barrier for the exchange of gases and additionally prevents the growth of bacteria, fungi, or other pathogens.[32] Improved barrier properties of cellulose can aid in maintaining the quality of the food and increase the shelf life without supplemental chemical preservers, etc. When a composite film packaging has low oxygen permeability coefficients, the oxygen pressure inside the container drops to the point where the oxidation is retarded, extending the shelf life of the food product. Furthermore, the water vapor permeability (water vapor transmission rate) for the packaged food products is of great importance for maintaining or extending the shelf life. Water vapor transmission rate indicates the amount of water vapor that permeates per unit of area and time in packaging materials. It is very important to avoid dehydration for bakery or delicatessen fresh foods, so it is necessary to avoid water permeation. ZnO/sodium cellulose showed great structural stability (Figure 8) that decreased the permeability owing to increase in crystallinity of the composite. These results matched the reported results on polyethylene/poly(ethylene-propylene) that showed a decrease in permeability with the increase in crystallinity.[33]

Table 2. Barrier properties of cellulose, sodium cellulose, and its composite.

Sample	Air permeability	Water vapor permeability
	(cm^3/ (m^2/Pa S))	(g/m s Pa)
Cellulose	1.05	4.68 $\times 10^{-9}$
Sodium cellulose	1.15	4.12 $\times 10^{-9}$
ZnO/sodium cellulose	0.137	2.44 $\times 10^{-9}$

2.3. Conclusions

For the first time, ZnO/sodium cellulose composite was synthesized by using zinc acetate and microwaves as a heating source. The XRD pattern of the ZnO/sodium cellulose composite showed a pattern corresponding to sodium cellulose with additional peaks of ZnO. The survey spectrum of the ZnO/sodium cellulose composite showed a peak corresponding to Na^+ ions. The morphology and microstructure of the ZnO/sodium cellulose composite showed the growth of irregular needle-like ZnO crystals on the sodium cellulose with the presence of sodium ions. Furthermore, thermal analysis suggested that Zn ions were incorporated into the sodium cellulose matrix and created a strong linkage bond. Temperature and permeability parameters are of crucial importance for food quality preservation, especially in real-life situations like food markets and household long-life use. ZnO/sodium cellulose can be employed as an innovative solution to satisfy the most important packaging requirements such as permeability, thermal resistance, low cost, and recyclability.

3. Experimental

3.1. Chemicals

All chemicals used in this study were of analytical grade and were purchased from Sigma-Aldrich. Cotton linter (DP = 900–920) was purchased from Sigma.

3.2. Preparation of the sodium cellulose

Sodium cellulose was prepared by immersing cotton linter in 20% NaOH for 3 h at room temperature. The sample was used without being washed in water and it was labeled as "sodium cellulose".

3.3. Preparation of the ZnO/sodium cellulose composite

Sodium cellulose (0.64 g, 0.013 mol) was immersed in 10% NaOH, followed by the addition of zinc acetate (0.05 mol). The mixture was then heated in a microwave oven (CEM Discover Synthesis Unit, CEM Corp., USA) under continuously focused microwave power that ranged from 0 to 800 W at 2.45 GHz. The reactions were performed in a 50-mL round-bottom Teflon tube, and the reaction temperature inside the flask was monitored using an integrated calibrated infrared temperature sensor.[5] The reaction temperature was increased from room temperature to 100 °C and was held for various lengths of time (10, 20, or 30 min). The produced composite was washed well until neutralization with water to remove the excess of sodium hydroxide and zinc acetate.

3.4. Characterization of composite

The FT-IR spectra of the prepared samples were measured by using a Bruker FT-IR IFS 66 spectrophotometer to investigate the physical structure of the processed composite. XRD patterns were measured using a Shimadzu Lab XRD-6000 with $CuK_{\alpha} = 1.5406$ Å radiation and a secondary monochromator. The XRD tube was operated at voltage of 30 kV and current of 30 mA in the 2θ range from 10° to 60°. The XPS spectrum of the composite was obtained with a Thermo Scientific K-alpha XPS instrument. A monochromatic Al K_{α} X-ray source was used for all the samples, and the pressure in the analysis chamber was 10^{-8} Pa. The resolution function of the instrument was found to have a width of 0.35 eV using the silver Fermi edge. The conditions used for all the survey scans were as follows: an energy range of 1360 to 0 eV, a pass energy of 200 eV, a step size of 0.7 eV, a sweep time of 180 s, and a circular X-ray spot with a diameter of 200 µm. For the high-resolution spectra, an energy range of 40 to 20 eV was applied, depending on the peak being examined, with a pass energy of 10 eV and a step size of 0.1 eV. All the spectra were analyzed using Avante data system software version 3.10 (Thermo Scientific Instruments). The morphology of the samples was evaluated using field emission scanning electron microscopy (FESEM) images obtained on an FESEM JEOL 6340 electron microscope equipped with an energy-dispersive X-ray (EDX) analysis instrument to investigate the elemental composition of the system. The UV-Vis spectrum of the prepared composite was measured using a double-beam spectrophotometer fitted with an integrating sphere (Shimadzu UV 3600). The composite fibers were compressed and were positioned across the face of the entrance slit of the spectrophotometer to ensure real and accurate data collection. The measurements were conducted at wavelength intervals of 1 nm from 200 to 800 nm. The thermal stability of the composite was investigated using a nonisothermal method on a Shimadzu DTA 50. In a real experiment, 7.0 mg was put in a covered aluminum crucible and heated at 15 K/min from 30 to 350 °C. Moreover, we used an empty aluminum pan as a reference, and both sample and reference were put in nitrogen gas flow at a constant rate of 60 mL/min to extract the gases emitted by the reaction. The glass transition temperature (T_g), the onset temperature of crystallization (T_c), the peak temperature of crystallization (T_p), and thermal stability (T) were determined.

3.5. Permeability study

The measurements were carried out in accordance with the TAPPI 2014 standard, with water vapor transmission rate of paper and paperboard at 23 °C and 50% RH. This technique runs for gravimetric determination of the water vapor transmission rate (WTVR) of both cellulose and its composite. WTVR is calculated from the following equation:

$$WVTR = \frac{24\ x}{A\ y},$$

where x is the mass gain in grams over time, y is the time in hours for gain x, and A is the exposed area in m^2.

The air permeability of the cellulose, sodium cellulose, and ZnO/sodium cellulose composite was measured according to the ISO 5636 standard. The measurements were achieved on samples with an area of 9.6 cm^2 under ambient air conditions, with a vacuum of 2.5 kPa. The volume of water that runs in the catch tank is collected after 10 min:

$$Ip = \frac{V}{A\,t\,\Delta P},$$

where I_p is the index of permeability, V is the volume in cm^3, A is the area in m^2, t is the time in s, and D_P is the change in pressure in Pa.

Acknowledgments

This article contains the results of a research project funded by King Abdelaziz City for Science and Technology (KACST) Grant No. LGP-37-90. The authors acknowledge Professor Ibrahim Bader at Ain Shams University and Dr Hisham Salah at King Khalid University for performing XPS and FT-IR analyses, respectively.

References

1. Ashby, M. F.; Bréchet, Y. J. M. *Acta Mater.* **2003**, *51*, 5801-5821.
2. Keshk, S. M. A. S.; El-Zahhar, A. A.; Bondock, S. *Starch* **2018**, *2018*, 1800035.
3. Gouda, M.; Keshk. S. M. A. S. *Carbohydrate Polymers* **2010**, *80*, 504-512.
4. Keshk, S. M. A. S.; Al-Sehemi, A. G. *Am. J. Polymer Sci.* **2013**, *3*, 46-51.
5. Keshk, S. M. A. S.; Hamdy, M.; Bader, I. *Am. J. Polymer Sci.* **2015**, *5*, 24-29.
6. Granqvist, C. G.; Niklasson, G. A.; Azens, A. *Appl. Phys. A* **2007**, *89*, 29-35.
7. Gallon, H. J.; Tu, X.; Twigg, M. V.; Whitehead, J. C. *Appl. Catal. B* **2011**, *106*, 607-616.
8. Espitia, P. J. P.; Otoni, C. G.; Soares, N. F. F. In *Antimicrobial Food Packaging*; Barros-Velazquez, J., Ed. Elsevier Academic Press: Cambridge, MA, USA, 2016, pp. 425-431.
9. Arrieta, M. P.; López, J.; López, D.; Kenny, J. M.; Peponi, L. *Polymer Degradation and Stability* **2010**, *95*, 2126-2146.
10. Ko, H.; Mun, S.; Min, S.; Kim, G.; Kim, J. *Materials* 2014, *7*, 7000-7009.
11. Sun, Q.; Su, Y.; Ma, X.; Wang, Y.; Jiang, Z. *J. Membrane Sci.* **2006**, *285*, 299-302.
12. Jia, N.; Li, S. M.; Ma, M. G.; Sun, R. C. *Mater. Lett.* **2012**, *68*, 44-46.
13. Calizo, I.; Alim, K. A.; Fonoberov, V. A.; Krishnakumar, S.; Shamsa, M.; Balandin, A. A.; Kurtz, R. In *The International Society for Optical Engineering 2007 Proceedings of SPIE 6 February 2007, Quantum Dots, Particles, and Nanoclusters IV*, 64810N. doi: 10.1117/12.713648.

14. Rajasudha, G.; Shankar, H.; Thangadurai, P. *Ionics* **2010**, *16*, 839-848.
15. Al-Sehemi, A. G.; Al-Shihri, A. S.; Kalam, A.; Du, G.; Ahmad, T. *J. Mole. Struct.* **2014**, *1058*, 56-61.
16. Ma, M. G.; Qing, S. G.; Li, S. M.; Zhu, J. F.; Fu, L. H.; Sun, R. C. *Carbohydr. Polym.* **2013**, *91*, 162-168.
17. El-Kemary, M.; Nagy, N.; El-Mehasseb, I. *Mater. Sci. Semicond. Process* **2013**, *16*, 1747-1752.
18. Mansikkamaki, P.; Lahtinen, M.; Rissanen, K. *Cellulose* **2005**, *12*, 233-242.
19. Gwon, J. G.; Lee, S. Y.; Doh, G. H.; Kim, J. H. *J. Appl. Polym. Sci.* **2010**, *116*, 3212-3215.
20. Yue, Y.; Gungping, H.; Qinglin, W. *Bioresources* **2013**, *8*, 6460-6463.
21. Ni, X. M.; Zhao, Q. B.; Li, B. B.; Cheng. J.; Zheng, H. G. *Solid State Commun.* **2006**, *137*, 585-588.
22. Ovshinsky, S. R.; Fetcenko, M. A.; Ross, J. *Science* **1993**, *260*, 176-181.
23. Dinand, E.; Vignon, M.; Chanzy, H.; Heux, L. *Cellulose* **2002**, *9*, 7-18.
24. Knill, C., Kennedy, J. *Carbohydr. Polym.* **2003**, *51*, 281-300.
25. Keshk, S. M. A. S. *Carbohydr. Polym.* **2015**, *115*, 658-662.
26. Lili, W.; Youshi, W.; Yuanchang, S.; Huiying, W. *Rare Metals* **2006**, *25*, 68-73.
27. Keshk, S. M. A. S.; Salah, H.; Hamdy, M.; Badr, I. In *World Academy of Science Proceedings of 18th International Conference on Applied Chemistry*; 12 January 2016; Zurich, Switzerland.
28. Joshi, A. G.; Sahai, S.; Gandhi, N.; Krishna, Y. G. R.; Haranath, D. *Appl. Phys. Lett.* **2010**, *96*, 123102-123103.
29. Ul-Islam, M.; Khattak, W. A.; Ullah, M. W.; Khan, S.; Park, J. K. *Cellulose* **2014**, *21*, 433-447.
30. Bagheri, M.; Rabieh, S. *Cellulose* **2013**, *20*, 699-705.
31. Keshk, S. M. A. S.; Syef, A. F. A.; El-Zahhar, A. A.; Yousef, S.; Bondock, S. *Transylvanian Review* **2018**, *16*, 7609-7619.
32. Deepansh, S.; Daljeet, S. D. *J. Appl. Pharma. Sci.* **2016**, *6*, 220-226.
33. Kofinas, P.; Cohen, R. E.; Halasa, A. F. *Polymer* **1994**, *35*, 1229-1235.